Published in final edited form as:

Acta Physiol (Oxf). 2020 July ; 229(3): e13460. doi:10.1111/apha.13460.

Massage as a mechanotherapy promotes skeletal muscle protein and ribosomal turnover but does not mitigate muscle atrophy during disuse in adult rats

Marcus M. Lawrence[1], **Douglas W. Van Pelt**[2,3], **Amy L. Confides**[2,3], **Emily R. Hunt**[2,3], **Zachary R. Hettinger**[2,3], **Jaime L. Laurin**[1], **Justin J. Reid**[1], **Frederick F. Peelor III**[1], **Timothy A. Butterfield**[3,4], **Esther E. Dupont-Versteegden**[2,3,*], **Benjamin F. Miller**[1]

[1]Aging and Metabolism Research Program, Oklahoma Medical Research Foundation, Oklahoma City, OK 73104, USA.

[2]Department of Physical Therapy, University of Kentucky, Lexington, KY 40536, USA.

[3]Center for Muscle Biology, University of Kentucky, Lexington, KY 40536, USA

[4]Department of Athletic Training and Clinical Nutrition, University of Kentucky, Lexington, KY 40536, USA.

Abstract

Aim: Interventions that decrease atrophy during disuse are desperately needed to maintain muscle mass. We recently found that massage as a mechanotherapy can improve muscle regrowth following disuse atrophy. Therefore, we aimed to determine if massage has similar anabolic effects when applied during normal weight bearing conditions (WB) or during atrophy induced by hindlimb suspension (HS) in adult rats.

Methods: Adult (10 month) male Fischer344-Brown Norway rats underwent either hindlimb suspension (HS, n=8) or normal weight bearing (WB, n=8) for 7 days. Massage was applied using cyclic compressive loading (CCL) in WB (WBM, n=9) or HS rats (HSM, n=9) and included four 30-minute bouts of CCL applied to gastrocnemius muscle every other day.

Results: Massage had no effect on any anabolic parameter measured under WB conditions (WBM). In contrast, massage during HS (HSM) stimulated protein turnover, but did not mitigate muscle atrophy. Atrophy from HS was caused by both lowered protein synthesis and higher degradation. HS and HSM had lowered total RNA compared with WB and this was the result of

*Corresponding author: Esther E. Dupont-Versteegden, College of Health Sciences, University of Kentucky, 900 S. Limestone CTW210E, Lexington, KY 40536-0200, Phone: 859-218-0592, eedupo2@uky.edu.

Author contributions

All experimentation was performed at the University of Kentucky, except for the analysis of protein and RNA synthesis and western analyses, which was performed at the Oklahoma Medical Research Foundation. M.L. was responsible for acquisition, analysis, and interpretation of data, and drafting and revising the manuscript. B.M. was responsible for acquisition, analysis and interpretation of data and for critically revising the manuscript. D.v.P., A.C., E.H., Z.H., J.L., J.R., and F.P. were responsible for acquisition, analysis and interpretation of data; T.B. and E.D.V. were responsible for conception and design of the experiments, for interpretation of the results and drafting and revising the manuscript. All authors have approved the final version of the manuscript and agree to be accountable for all aspects of the work. All persons designated as authors qualify for authorship, and all those who qualify for authorship are listed.

Conflict of Interest

The authors declare that they do not have any competing interests associated with this work.

significantly higher ribosome degradation in HS that was attenuated in HSM, without differences in ribosomal biogenesis. Also, massage increased protein turnover in the non-massaged contralateral limb during HS. Finally, we determined that total RNA degradation primarily dictates loss of muscle ribosomal content during disuse atrophy.

Conclusion: We conclude that massage is an effective mechanotherapy to impact protein turnover during muscle disuse in both the massaged and non-massaged contralateral muscle, but it does not attenuate the loss of muscle mass.

Keywords

Cross-over effect; disuse atrophy; protein turnover; ribosome biogenesis; ribosome turnover

Introduction

Skeletal muscle loss is a common consequence of conditions associated with abrupt inactivity, such as major surgery to a joint, immobilization due to fracture, or extended bed rest from illness.[1,2] Changes in both protein synthesis and protein degradation contribute to muscle loss during disuse atrophy, even though their relative contributions are debated.[3,4] Skeletal muscle atrophy due to disuse is associated with a decrease in protein synthesis[5–10] and creates a state in which the muscle becomes resistant to anabolic stimuli,[11] such as amino acids.[12] Measurements of protein degradation under atrophying conditions are technically challenging, but studies of markers indicate an upregulation of calpains,[13,14] apoptosis,[13,15,16] the autophagy-lysosomal system,[17,18] nuclear factor-kappaB signaling,[19] and the ubiquitin-proteasome pathway.[5,16,20] Collectively, these findings suggest that muscle atrophy from disuse has contributions from both reduced protein synthesis and elevated degradation.

Strategies to minimize the loss of skeletal muscle protein during disuse may not be the same as those that stimulate hypertrophy since pathways to counteract muscle loss are not simply opposite. For instance, muscle loss during disuse happens rapidly with a 3.5% loss of quadriceps muscle cross sectional area (CSA) with just 5 days of immobilization in young human subjects,[21] which far exceeds physiological hypertrophic responses. In addition, in at least one case, a resistance training protocol that was effective at inducing muscle hypertrophy was not effective at preventing muscle loss in adult rodents.[22] In clinical settings, methods and techniques used to increase muscle mass (such as heavy resistance training) might not be feasible during a period of immobilization or disuse and therefore alternative interventions are needed to prevent muscle atrophy and stimulate muscle growth.

We recently showed that massage is an effective mechanotherapy to improve recovery from disuse atrophy in adult rats.[23] Multiple bouts of massage applied during the reloading/regrowth period enhanced cumulative protein synthesis and muscle fiber cross sectional area (CSA) compared to reloading in the absence of massage. Interestingly, these effects had a cross-over effect to the contralateral non-massaged limb as well. Consequently, we speculated whether massage could also be applied during the period of muscle disuse to minimize muscle loss. Furthermore, we found that a single massage treatment to unperturbed muscle acts as an immunomodulatory stimulus in both the massaged limb and

the contralateral non-massaged limb,[24] but we did not measure anabolic responses. Additionally, we recently found that a single acute bout of massage in unperturbed adult rat muscle stimulated mechanosensitive signaling and remodeling, without affecting protein synthesis or muscle mass.[25] However, in addition to the snap-shot protein markers assessed 24 hours after the massage bout, the protein synthesis measurement utilized shows bias towards proteins that are the most abundant or have the fastest synthesis rates.[26] Thus, similar to our previous work with multiple massage bouts, assessment of long-term (days) protein turnover (synthesis and degradation), allows for greater insight into the total protein pool. Moreover, it is currently unknown if multiple bouts of massage will also affect anabolic pathways under normal ambulatory conditions or if muscle homeostasis needs to be perturbed for massage to show growth-related responses. As such, previous studies demonstrate that anabolic stimuli in muscle, such as amino acid supplementation, are less effective in the absence of some form of mechanical loading.[27] Thus, further investigations are needed to determine if multiple bouts of massage has a positive influence on muscle mass and protein synthesis during long-term unperturbed and disuse periods.

Previous work from our lab found that massage was associated with mechanosensitive signaling.[23,25] In particular, a single acute bout of massage in adult rat muscle stimulated integrin-like kinase signaling with unchanged muscle mass in 24 hours[25]. Moreover, multiple bouts of massage during reloading stimulated muscle regrowth and augmented integrin mRNA expression (specifically, α−7 integrin or Itg7a, one of the most abundant integrins in muscle) and phosphorylation of FAK.[23] However, it is unknown how multiple bouts of massage effects these same intracellular signaling pathways during normal ambulatory weight bearing and during a period of disuse.

It is well established that mTORC1 and its downstream targets also influence skeletal muscle mass through modulating ribosome biogenesis.[28–30] Ribosomes control translation of proteins, and an increase in ribosomal accumulation is thought to influence protein synthesis and muscle growth.[31–33] Ribosomal accumulation is suggested to be mainly regulated by *de novo* ribosome synthesis.[34,35] In addition to mTORC1 pathway proteins, RNA Pol I transcription, an essential component of ribosomal biogenesis, is regulated by transcription factors, including upstream binding factor (UBF) and c-myelocytomatosis oncogene (c-Myc).[32] Total RNA content, an indicator of ribosomal content, increases in response to muscle growth stimuli including resistance exercise and functional overload[32,33,36–38] and is also associated with increases in protein synthesis[33,36,39]. In contrast, during muscle atrophy from disuse or denervation, total RNA decreases[40–45] and is associated with decreased protein synthesis.[44,45] In the present study, we use our established methods that measure ribosomal biogenesis[39,46,47] in conjunction with mathematical modeling,[23,26] to further understand the influence of unloading and mechanical loading on the regulation of ribosomal content and to determine changes that occur during conditions of muscle loss.

The goals of the present study were to determine [1] if massage in the form of cyclic compressive loading (CCL) has an anabolic effect on muscle when applied during normal ambulatory weight bearing (WB), or [2] during atrophy induced by hindlimb suspension (HS), and [3] if massage induces a cross-over effect in the contralateral limb as observed

during reloading. To provide mechanistic insight into the potential beneficial effects of massage we measured ribosome biogenesis and muscle protein synthesis as well as calculated ribosome degradation and muscle protein degradation. We hypothesized that massage applied during WB increases ribosome biogenesis, muscle protein synthesis, and muscle fiber CSA, whereas, massage applied during HS protects against muscle fiber CSA loss by stimulating ribosome biogenesis and muscle protein synthesis, and decreasing ribosome and muscle protein degradation. Finally, we hypothesized that massage during WB or HS would also have positive effects on the contralateral non-massaged limb.

Results

Anabolic and signaling effects of massage during WB

In unperturbed weight bearing conditions, multiple bouts of massage had no effect on the synthesis of myofibrillar (Fig. 2a) or cytosolic (Fig. 2b) proteins. These results were mirrored by a lack of difference in RNA concentration (Fig. 2c), total RNA (Fig. 2d), and ribosomal biogenesis (total RNA FSR, Fig. 2e) with massage application. Furthermore, no differences were observed between WB and WBM for gastrocnemius muscle wet weights (Fig. 2f), wet weight to body weight ratio (Fig. 2g), body weights (Fig. 2i), fiber type specific CSA (Table 1), or fiber-type distribution (Table 2). Fiber size frequency distribution for CSA showed significantly fewer fibers in the 2500 μm^2 size range in WBM compared to WB, with no differences in any other fiber size range (Supplemental Fig. 1) and similarly, no difference for mean fiber CSA was observed with massage in weight bearing rats (Fig. 2h). Also, massage had no significant effect on levels of intracellular signaling proteins involved in the regulation of anabolic processes such as protein translation, proteasomal degradation, ribosome biogenesis (Table 3).

Effects of massage on anabolic pathways during HS

To highlight the clinical relevance of HS-induced atrophy and the potential therapeutic benefit of massage, we expressed our anabolic measurements of HS and HSM as a percent (%) difference from the WB control group. For complete transparency, we also provide the absolute values of HS and HSM (Supplemental Fig. 2 & 3), which mirror the percent difference from WB values. Importantly, HSM had a significantly lower percent difference from WB in myofibrillar protein synthesis rate (K_{syn}, mg day^{-1}) compared to HS (Fig. 3a). However, HSM was not different from HS for myofibrillar protein degradation rate (K_{deg}, 1/t) (Fig. 3b). Cytosolic protein turnover did not follow the same pattern as myofibrillar, such that HSM was not significantly different than HS for cytosolic protein synthesis rate (Fig. 3c). Furthermore, massage was associated with a significant attenuation of cytosolic protein degradation (Fig. 3d).

No significant differences were observed between HS and HSM for RNA concentration (Fig. 3e), total RNA (Fig. 3f), or ribosome biogenesis (RNA K_{syn}) (Fig. 3g). In contrast, ribosomal degradation rate (RNA K_{deg}) was significantly lower in HSM compared to HS (Fig. 3h). Also, HS and HSM were not significantly different for muscle wet weight (Fig. 3i), wet weight to body weight ratio (Fig. 3j), mean fiber CSA (Fig. 3k), body weights (Fig. 3l), fiber type specific CSA (Table 1), or fiber-type distribution (Table 2). Furthermore, there

were no significant differences in the total and phosphorylated protein levels for Akt, FOXO3A, ERK1/2, eEF2, 4EBP1, S6K1, rpS6, and UBF-1, or total MuRF1 between HSM and HS (Table 3). HSM displayed significantly greater c-Myc expression than HS (Table 3).

Cross-over anabolic and signaling effects of massage during WB

In unperturbed weight bearing rats no significant differences were observed in the left non-massaged muscle (WBM-L) from animals who received massage in their right limb compared to the right limb in animals who did not receive massage (WB) for the following variables: myofibrillar (Fig. 4a) and cytosolic (Fig. 4b) protein synthesis, RNA concentration (Fig. 4c), total RNA (Fig. 4d), ribosome biogenesis (RNA FSR, Fig. 4e), gastrocnemius wet weight (Fig. 4f), wet weight to body weight ratio (Fig. 4g), mean fiber CSA (Fig. 4h), fiber type specific CSA (Table 1), or fiber type distribution (Table 2). Similarly, no significant difference was observed between WBM-L and WB for total or phosphorylated protein expression for FOXO3A, FAK, ERK1/2, eEF2, 4EBP1, and rpS6, or total MuRF-1 (Table 3). WBM-L had significantly lower total Akt and greater total S6K1 and UBF-1 compared to WB alone, with no differences in phosphorylated Akt, S6K1, or UBF-1 (Table 3).

Cross-over anabolic and signaling effects of massage during HS

Similar to the massaged limb, the contralateral non-massaged left limb (HSM-L) in the animals that received massage, had significantly greater myofibrillar protein synthesis rate compared to the right limb of animals that did not receive massage (HS) (Fig. 5a). However, no differences were observed between HSM-L and HS for the myofibrillar protein degradation rate (Fig. 5b). Similarly, there were no differences in the cytosolic protein synthesis rate (Fig. 5c) between HSM-L and HS, but HSM-L had significantly lower cytosolic protein degradation rate compared to HS (Fig. 5d). Furthermore, HSM-L had a significantly lower RNA concentration (Fig. 5e) compared to HS, but no differences in total RNA (Fig. 5f) or ribosome biogenesis (Fig. 5g). In contrast to the right massaged limb, the left non-massaged contralateral muscle displayed significantly greater ribosomal degradation compared to HS (Fig. 5h). Furthermore, gastrocnemius wet weight (Fig. 5i), wet weight to body weight ratio (Fig. 5j), mean fiber CSA (Fig. 5k), fiber type specific CSA (Table 1), and fiber type distribution (Table 2) were not different in the left non-massaged limb in the massaged rat compared to HS alone. Finally, total or phosphorylated protein levels of Akt, FOXO3A, FAK, ERK1/2, eEF2, S6K1, 4EBP1, UBF-1, and total c-Myc or MuRF-1 were not different between HSM-L and HS (Table 3), but HSM-L displayed significantly greater phosphorylated rpS6 levels compared to HS, with no differences in total rpS6.

Discussion

The primary finding of this study is that massage is an effective mechanotherapy to stimulate muscle protein and ribosomal turnover during disuse, although it did not prevent the loss of muscle mass. With massage there was greater myofibrillar protein synthesis and an inhibition of cytosolic protein degradation in unloaded muscle. In contrast, massage during weight-bearing conditions does not promote muscle hypertrophy, protein synthesis, or ribosome biogenesis. This present study further shows that disuse atrophy is caused by a combination of decreased protein synthesis and increased protein degradation. We also

showed for the first time that loss of ribosomal content during disuse atrophy is primarily dictated by elevated ribosomal RNA degradation, rather than lowered ribosomal RNA synthesis. In addition, massage attenuated the elevated ribosomal degradation during disuse. Finally, massage during HS had significant cross-over effects on the contralateral non-massaged limb, including a greater myofibrillar protein synthesis and attenuated cytosolic protein degradation. Collectively, these results indicate that massage is an effective protein and ribosomal turnover stimulus during disuse atrophy and can benefit the limb contralateral to the massaged muscle. However, massage during either a period of disuse or normal loading had no hypertrophic effects, suggesting that a different massage dosage or combination with another therapeutic intervention may be needed to increase muscle mass and size. Future work should determine if the robust protein and ribosomal turnover stimulated by massage during disuse atrophy maintains myofibrillar protein quality and/or muscle function.

Protein turnover during disuse atrophy with and without massage

The results from this study strongly suggest that disuse induced-muscle loss in rats is caused by both a decrease in protein synthesis and an increase in protein degradation, which agrees with previous work from our lab[23] and others.[48] Important for this study was to be able to make direct measures, not markers, of protein synthesis and degradation. Stable isotope measurements during a period of muscle loss are complicated by non-steady state conditions of the muscle. Specifically, an important assumption for stable isotope tracer measurements is that the protein pool size is constant.[49] During muscle loss, this condition is violated because the size of the muscle, and therefore the protein pool of measurement, decreases over time during the experimental period. Therefore, we developed a modeling approach, [23,26] similar to others,[48] that could account for changes in pool size during non-steady state conditions. From this approach we were also able to calculate both synthesis and degradation to assess both aspects of protein turnover. The calculated protein degradation rate in this study was higher than our previous study with HS and massage[23] and also differs from a study in which no increase in degradation was reported.[48] The current study measured turnover rates during the initial period of unloading (7 days), while our previous study measured turnover rates over 14 days of unloading and the study of Bedermen and colleagues measured degradation from days 8 through 21 of unloading.[23,48] The timing of measurement is important for two reasons. The first is that there is an initial “adaptive phase” of unloading that has been described as occurring between 3–7 days of HS.[50] Our labeling period in the current investigation captures the adaptive phase, while the study of Bedermen et al. (2015) does not. Second, our previous study and the work of Bedermen and colleagues has a slightly longer measurement period compared to the current study, which like measurements of synthesis, will have an increasing contribution of proteins that turn over at a slower rate.[26] In combination, the three studies highlight potential differences in the contribution of protein degradation to muscle atrophy in the acute (0–7 days) versus the chronic phase (>7 days) of muscle disuse.

Muscle fiber size is predominantly controlled by changes in the turnover of myofibrillar proteins and our novel data demonstrate that massage has positive effects on myofibrillar protein turnover without mitigating muscle loss during disuse-induced muscle atrophy.

Specifically, the lack of preservation of muscle size with massage (HSM) during atrophy coincided with greater myofibrillar protein synthesis with no changes in myofibrillar degradation. Of note, the lack of change in myofibrillar degradation rates with massage during disuse was compared to a state where degradation was already elevated, namely HS. Our previous study[23] found that with massage there were higher myofibrillar degradation rates during reloading following HS, which indicated increased muscle remodeling. Our current study further supports our previous findings that massage is a potent stimulus to augment myofibrillar protein synthesis. However, unlike our previous study in which massage resulted in greater muscle regrowth during reloading (Miller et al, 2018), massage during a period of disuse had no effect on muscle size. This finding highlights that a period of disuse results in a powerful muscle atrophy event that requires an even greater myofibrillar turnover stimulus than what was seen herein to preserve muscle mass and size. The inability of massage to attenuate muscle atrophy despite robust myofibrillar protein turnover could mean that massage improved/maintained myofibrillar protein quality and thus potentially maintained muscle function. We did not measure muscle function in the current investigation, but previous work from our lab found that massage maintains muscle function compared to no massage following damaging eccentric contractions.[51–54] Also, future work should determine whether a different dose or frequency of massage could have a greater effect during a period of disuse and if there are other potential interventions that could be combined to enhance the anabolic effect of massage as a mechanotherapy.

Massage also affected cytosolic protein turnover during disuse. Most cytosolic proteins are regulatory in nature and influence key pathways including energy balance, metabolism, and proteostasis. Our novel data showing lower cytosolic degradation with massage suggest a specific effect on turnover of cytosolic proteins during a disuse period, but it is currently unknown what the identity of these proteins are. Cytosolic proteins are extremely heterogeneous and future work should use a proteomics approach to determine the specific proteins affected by massage, including the turnover and change in content of each protein.

Ribosome turnover during disuse atrophy with and without massage

Ribosomal content is often used as an indicator of ribosomal biogenesis.[45,55,56] However, an unexpected finding of the current study was that lowered ribosome content during disuse atrophy was not paralleled by downregulation of ribosome biogenesis, but rather was driven by a dramatic upregulation in ribosome degradation. The finding that total RNA content (or RNA concentration) did not reflect ribosome biogenesis clearly demonstrates that assessing ribosome content by itself may hide the dynamic processes of ribosome turnover, as is the case for measurements of protein content. If we had only measured ribosomal content during HS with and without massage, we would have concluded that ribosomal biogenesis was lowered with atrophy. However, our isotope measurements indicate that this is clearly not the case as evidenced by minimal changes in ribosome biogenesis during HS and HSM compared to WB. Instead, the decreased ribosomal content was caused by dramatically elevated levels of ribosomal degradation (~600% in HS) without a change in ribosomal synthesis. Because total RNA content was heavily influenced by the loss in muscle mass, we also calculated RNA degradation rates using RNA concentration, which still resulted in a dramatic increase of ~260% in HS compared to WB, further supporting our RNA

degradation rates calculated with total RNA. Lastly, the disconnect between signaling pathways regulating ribosome biogenesis (e.g., mTORC1 pathway proteins, c-Myc, and UBF-1) and our data on actual rates of ribosome biogenesis further emphasize the importance of directly measuring dynamic ribosome turnover.

The current study raises interesting questions about whether total ribosomal content or ribosomal biogenesis and degradation dictate anabolic or atrophy events. In previous studies, our lab[39,47] and others[57] have shown that increases in muscle protein synthesis rates are correlated with increases in ribosomal biogenesis in both rats[47] and humans.[39,57] We have further shown that protein synthesis rates do not correlate as well with ribosomal content as with ribosomal biogenesis,[39] although others have shown a relationship with ribosomal content.[38,58,59] In the current investigation, under conditions that lack a loading stimulus, there was not a significant correlation between myofibrillar protein synthesis and ribosome biogenesis ($r = -0.011$, $p = 0.961$, *data not shown*). Taken together, the ribosome and protein turnover findings indicate that during periods of growth, ribosome biogenesis and myofibrillar protein synthesis are related. However, during periods of disuse atrophy this relationship does not exist because ribosomal degradation is a prominent regulating factor. Further work is needed to tease out the exact contributions of dynamic ribosome biogenesis and degradation during various loading states in healthy and pathological conditions.

Anabolic intracellular signaling is largely unaffected by massage

In order to identify intracellular signaling pathways associated with the observed muscle protein turnover changes, we measured upstream (Akt, ERK1/2, FOXO3A) and downstream (eEF2, S6K1, 4EBP1, rpS6) markers of mTOR that can alter muscle protein turnover.[36] We also measured a marker of proteasomal protein degradation (MuRF1). Massage in general had no effect on mTOR-related or proteasomal degradation signaling in muscles undergoing atrophy with HS or during weight bearing. We compared HS and HSM to WB for phosphorylated and total FAK levels, and found that our present study is not in agreement with previous findings.[23,60] In particular, our lab[23] and others[60] have found that total FAK decreases during HS compared to WB. In the current study, we found no changes in phosphorylated FAK during HS or HSM compared to WB, which is agreement with our previous study's animals undergoing HS.[23] The differences in total FAK levels between our current investigation and previous findings[23] may be due to the application of either massage (HSM) or sham (HS) treatment, which required the animals to be briefly reloaded prior to anesthesia during the four separate 30 min. bouts. Nevertheless, both HS and HSM experienced significant reductions in muscle mass (Figure 3i) and size (Figure 3k) compared to WB.

Massage was associated with signficantly higher c-Myc expression in animals undergoing HS. However, no changes were observed in phosphorylated protein level of S6K1, or in ribosome biogenesis (which c-Myc regulates) questioning the significance of increases in c-Myc total protein level. Important to note, we collected muscle tissues 24 hours after the last bout of massage, similar to our previous work,[23] which may have been too late to observe changes in acute intracellular signaling which usually occur sooner after a mechanical

stimulus.[61,62] Future work should determine the acute (minutes to hours) anabolic signaling response to massage.

Cross-over effect of massage during normal loading and hindlimb suspension

Massage during HS had a cross-over effect in the contralateral non-massaged gastrocnemius muscle (HSM-L), which included greater myofibrillar protein synthesis and attenuated cytosolic protein degradation, with no effect on mitigating muscle loss. In addition, HSM-L had significantly higher phosphorylated rpS6 levels compared to HS alone, which may indicate greater translational efficiency,[36] a finding that was not observed in the massaged limb. The differences in phosphorylated rpS6 levels between the massaged limb and non-massaged limb suggests that the mechanisms by which myofibrillar protein synthesis was elevated were likely different between the two legs, similar to our previous work.[23] Also, HSM-L had no differences in ribosome biogenesis and a higher ribosome degradation rate, in contrast to the massaged muscle which had lower ribosome degradation compared to HS alone. Therefore future work understanding the acute anabolic signaling regulating protein and ribosomal turnover in the contralateral non-massaged is needed.

The cross-over effect from mechanical stimuli such as unilateral resistance exercise is well documented in terms of transferring muscle strength,[63–65] but only few studies have reported an effect on muscle mass during disuse as recently reported in a study and a review from the same group.[66,67] Importantly, to the best of our knowledge, our recent work[23] and current study provide the only cross-over effects reported on dynamic protein turnover induced by mechanical stimulation. Specifically, our previous work showed that massage stimulates a cross-over effect in the contralateral non-massaged muscle of enhanced myofibrillar turnover and greater muscle regrowth following a period of disuse atrophy, which was identical to the massaged limb.[23] Similarly, our current data show similar cross-over effects between the massaged limb and contralateral non-massaged limb of enhanced myofibrillar turnover and unaffected muscle loss during a period of disuse. Thus, mechanical stimulation provides a potential therapeutic cross-over effect on muscle growth by stimulating protein turnover. Moreover, we previously found that massage applied during undisturbed loading resulted in load-dependent changes in immunomodulatory gene expression in the massaged limb, whereas changes in the contralateral non-massaged limb were load-independent.[24] The exact mechanisms responsible for the cross-over effect are unknown, but are considered to be either neurally mediated[68] or from factors released by the muscle (e.g. exosomes) that can act in an endocrine-like fashion[69]. In previous studies, the cross-over effect was specific to the same contralateral muscle that was manipulated including with unilateral resistance exercise[66] and our recent massage work.[23,24] We did not explore other muscles in the current study to confirm if this was true with massage during HS. Together, the current results provide evidence for alternative clinical interventions in individuals who may have unilateral pathologies that prevent mechanical manipulation of the affected limb. The optimal massage dosage used for positive effects on the non-massaged muscle should be determined.

Limitations

There are limitations to our current approach for measuring protein and RNA synthesis and degradation because of dynamic changes in protein content during atrophy. Consecutive measurements of RNA and protein content were not possible and therefore, we calculated a change in protein or RNA content instead of measuring it directly as has been performed in the past.[48] To confirm the robustness of our findings, we performed several different approaches to calculate changes in the average content as proxy of pool size. Namely, for protein turnover we used individual and average muscle mass values and for RNA turnover we utilized both RNA concentration (where HS and HSM were not significantly different than WB, *data not shown*) and total RNA (where HS and HSM were significantly lower than WB, *data not shown*) for our calculations. The end result was that all approaches agreed in both the directional change, as well as the degree of variability, giving us confidence in our results.

Conclusion

In summary, massage as a mechanotherapy during atrophy robustly enhanced myofibrillar protein synthesis and protected against ribosomal degradation, but could not overcome the muscle loss due to disuse. Further, the same positive effects on stimulating myofibrillar and cytosolic protein turnover were apparent in the contralateral non-massaged limb. To the contrary, massage during normal loading (WB) in rats did not positively affect any anabolic parameter assessed in either the massaged or contralateral non-massaged limb indicating that massage might only be effective when muscle is not in homeostasis. We also show that disuse atrophy from HS is caused by a combination of decreased protein synthesis and increased protein degradation. Importantly, we show for the first time that muscle total RNA content is lowered during disuse atrophy primarily by elevated ribosomal degradation, not reduced synthesis, and that the increase in degradation was attenuated by massage. These findings support the need for future work to determine if manipulating the massage dosage (load and/or frequency) or combining other potential interventions could enhance the anabolic effect of massage further to mitigate muscle loss during disuse or enhance muscle protein and ribosomal turnover and growth during an unperturbed state.

Materials and Methods

Ethical approval

All animal procedures were conducted in accordance with institutional guidelines for the care and use of laboratory animals and were approved by the Institutional Animal Care and Use Committee of the University of Kentucky, which operates under the guidelines of the animal welfare act and the public health service policy on the humane care and use of laboratory animals. The study was conducted in adherence to the NIH *Guide for the Care and Use of Laboratory Animals*. Further, all publication material submitted conforms with *Acta Physiologica's* good publishing practice in physiology.[70]

Study design and animal experimentation

Ten month old male Fischer 344/Brown Norway (F344BN) rats (National Institute on Aging, Bethesda, MD) were housed in a room, controlled for temperature and humidity, and kept on a 12:12 h light:dark cycle with *ad libitum* access to food and water within the Division of Laboratory Animal Resources at the University of Kentucky.

Random assignment of the rats was performed into one of four groups: weight bearing (WB; $n = 8$), weight bearing with massage (WBM; $n = 9$), hindlimb suspension for 7 days (HS; $n = 8$), and hindlimb suspension for 7 days with massage (HSM; $n = 9$). Seven days of HS was chosen to compare to our previous work where massage was applied over a 7 days reloading/regrowth period following atrophy.[23] We also chose 7 days of HS to test if massage could attenuate atrophy during the atrophy period, which typically stabilizes at ~14 days of HS.[5,59] Hindlimb suspension was performed as previously described by us.[71] Briefly, a tail device containing a hook was attached with gauze and cyanoacrylate glue while the animals were anesthetized with isoflurane (2% by inhalation). After the animal regained consciousness, the tail device was connected via a thin cable to a pulley sliding on a vertically adjustable stainless steel bar running longitudinally above a high-sided cage. The system was designed in such a way that the rats could not rest their hindlimbs against any side of the cage. For WBM and HSM rats, the massage mimetic CCL was applied to the right gastrocnemius muscle every other day starting on day 0 for a total of 4 bouts, as described in.[23]

All groups (WB, WBM, HS, HSM) received a bolus of (99%) deuterium oxide (D_2O) at the start of the experiment, equivalent to 5% of the body water pool, followed by drinking water enriched 8% with D_2O for the remainder of the 9 day period, as described in[23] (Figure 1). Rats in the HS and HSM group were hindlimb suspended 2 days after the initial D_2O injections, for 7 total days of suspension. Rats in the WBM and HSM underwent CCL (described below) 2 days after the initial D_2O injections for 4 total bouts. Twenty-four hours after the last bout of CCL for the WBM and HSM group or at designated time points (see Figure 1) for the other groups (WB and HS), rats were euthanized with sodium pentobarbital (i.p. injection, 150 mg g^{-1}) followed by exsanguination through cardiac puncture, as described in.[23] Blood was collected, clotted at room temperature for 30 min. and then centrifuged at 2000g for 10 min. at 4°C. Serum was then aliquoted and frozen at −80°C until analyses. Gastrocnemius muscles from both hindlimbs were quickly removed, trimmed of excess fat and connective tissues, weighed, and flash frozen in liquid nitrogen. Only the right gastrocnemius muscle was used for rats in the WB and HS group. Both the non-massaged left (WBM-L and HSM-L) and massaged right gastrocnemius muscles (WBM-R and HSM-R) were collected to be enable determination of effects of massage on the contralateral side in animals in which the right leg was massaged, as described in[23]. Gastrocnemius muscles were cut at the midbelly and the distal half was mounted for tissue sectioning in a cryostat to determine muscle fiber cross sectional area and for (immuno) histochemical analyses, as described in[23]. For determination of protein and RNA synthesis, total RNA abundance and Western blot analysis cross-sectional slides of about 50mg were cut at the mid-belly of the muscle ensuring equal representation from medial and lateral gastrocnemius.

CCL, a massage mimetic, of gastrocnemius muscle

CCL, the massage-mimetic, consisted of 30 minute bouts of mechanical loading over the gastrocnemius muscle at 4.5N load and 0.5Hz as described previously.[23,24] This specific CCL load (4.5N) in rats was previously determined to not cause any overt muscle damage.[24,72] To apply CCL, rats were anesthetized using isoflurane (5% induction, 2% maintenance isoflurane/500 ml oxygen via a nose cone) and placed left lateral recumbent on a heated sling with the right hindlimb secured to a small platform by tape encircling the talocrural joint. The lateral aspect of the gastrocnemius muscle was placed facing superiorly for the application of CCL by a custom fabricated CCL device as described previously.[23,25,51] A spring-loaded strut mechanism was designed to allow a cylinder to roll longitudinally over the contoured mass of the right gastrocnemius and displace vertically in response to the normal force exerted upwards from the tissue to the roller during an oscillating movement. A force transducer enabled continuous, real-time voltage output, calibrated to known loads, permitting tuning of the normal force applied to the roller. For CCL application, the roller was placed on the skin overlying the gastrocnemius muscle, immediately proximal to the lateral malleolus of the hind limb, and cycled proximal and distal along the length of the gastrocnemius muscle, compressing both the medial and lateral heads, for 30 minutes per bout at a frequency of 0.5 Hz. Rats in WB and HS group were anesthetized and placed lateral recumbent without application of CCL (sham treatment) for 30-minutes, as previously described in.[23,51] The CCL bout length of 30 minutes was determined from previous work by us in rabbits that this duration of CCL maintained muscle function following a damaging stimulus.[51] The 4 bouts of CCL every other day was determined from our recent publication, in which 4 bouts applied every other day during a 7 day reloading period following atrophy augmented muscle regrowth.[23] After the fourth and last bout of CCL or sham treatment, the rats were allowed to recover in their cages for 23.5 hours after which they were euthanized, as previously described in.[23] Rats had *ad libitum* access to food and water (i.e., not fasted) until euthanasia since the primary outcome of this study was to measure cumulative protein and ribosomal turnover (described below) over the entire intervention period.

Total RNA Isolation

As previously described in,[47] total RNA was isolated from a frozen section of muscle (~30–75mg) in 1ml Trizol (Thermo Fisher Scientific, Rockford, IL, USA) using a handheld homogenizer. The homogenate was centrifuged at 12,000g for 10 minutes at 4°C. The resulting supernatant was removed and 200μL of chloroform was added. The mixture was shaken by hand vigorously then centrifuged at 12,000g for 15 minutes at 4°C. The upper aqueous layer was isolated, mixed with 500μL of isopropanol, and then left to incubate at room temperature for 20 minutes. After incubation, the mixture was centrifuged at 12,000g for 10 minutes at 4°C to pellet RNA. The RNA pellet was isolated, rinsed with 1ml of 75% ethanol, and resuspended in 50μL of molecular biology grade H_2O. RNA integrity was assessed using the Agilent Bioanalyzer (Agilent Technologies, Santa Clara, CA, USA) and RNA concentration was determined using a Nano Drop (Thermo Fisher Scientific) to then calculate total RNA per mg muscle.[23,47]

Determination of protein and RNA fractional synthesis rate

Protein synthesis was determined according to methods described in.[23] Briefly, skeletal muscle tissue was homogenized 1:10 in isolation buffer (100mM KCl, 40mM Tris HCl, 10mM Tris Base, 5mM MgCl2, 1mM EDTA, 1mM ATP, pH = 7.5) with phosphatase and protease inhibitors (HALT, Thermo Fisher Scientific) using a bead homogenizer (Next Advance Inc., Averill Park, NY, USA). After homogenization, subcellular fractions were isolated via differential centrifugation as previously described.[23,73–75] Once protein pellets were isolated and purified, 250μl 1M NaOH was added and pellets were incubated for 15 min at 50°C while slowly mixing. Protein was hydrolyzed by incubation for 24 h at 120°C in 6N HCl. The pentafluorobenzyl-N,N-di(pentafluorobenzyl) derivative of alanine was analyzed on an Agilent 7890A GC coupled to an Agilent 5975C MS as previously described.[23,73–75]

A separate RNA isolation of ~15–25mg of frozen muscle was performed for ribosomal turnover analysis according to our previously published procedures.[23,39,46,47] We utilized Trizol for RNA isolation exactly the same as described above for Total RNA isolation. The isolated RNA was hydrolyzed overnight at 37°C with nuclease S1 and potato acid phosphatase. Hydrolysates were reacted with pentafluorobenzyl hydroxylamine and acetic acid and then acetylated with acetic anhydride and 1-methylimidazole. Dichloromethane extracts were dried, resuspended in ethyl acetate, and analyzed on an Agilent 7890A GC coupled to an Agilent 5975C MS. For GC-MS analysis, we used a DB-17 column and negative chemical ionization, with helium as the carrier and methane as the reagent gas. The fractional molar isotope abundances at m⁄z 212 (M0) and 213 (M1) of the pentafluorobenzyl triacetyl derivative of purine ribose were quantified using MassHunter software. All analyses were corrected for abundance with an unenriched pentafluorobenzyl triacetyl purine ribose derivative standard.[23,39,46,47]

To determine body water enrichment, 125μl of serum was placed into the inner well of o-ring screw cap and inverted on an 80°C heating block overnight. 2μl of 10M NaOH and 20μl of acetone were added to all samples and to 20μl 0–20% D_2O standards and then capped immediately, as previously described.[23,47] Samples were vortexed at low speed and left at room temperature overnight. Extraction was performed by the addition of 200μl hexane. The organic layer was transferred through anhydrous Na_2SO_4 into GC vials and analyzed via Electron Ionization (EI) mode.[23,47]

As previously described,[23,47] the newly synthesized fraction (f) of proteins was calculated from the enrichment of alanine bound in muscle proteins over the entire labelling period, divided by the true precursor enrichment (p), using plasma D_2O enrichment with MIDA adjustment.[23,47,76] Similarly, RNA synthesis (~85% of total RNA exists as ribosomal RNA) was determined by deuterium incorporation into purine ribose of RNA as previously published[39,46] with MIDA adjustment of the equilibration of the enrichment of the body water pool with purine ribose.

Modeling calculations to account for non-steady state conditions

Disuse atrophy is a non-steady state condition (i.e., rapid muscle loss), which violates an assumption of isotopic labeling. To account for potential non-steady state conditions, calculations were made based on our previous publications[23,26] using muscle protein synthesis rates and muscle mass or RNA synthesis rates and total RNA content. These calculations were only employed in the hindlimb suspended groups (HS or HSM), as this is considered a non-steady state condition, whereas the weight bearing groups (WB or WBM) were analyzed using standard steady state calculations (i.e., fractional synthesis rate, FSR). The mass of protein at time *t*, *P(t)*, obeys the differential equation:

$$\frac{\mathrm{d}P}{\mathrm{d}t} = k_{syn} - \quad k_{deg}P(t), \tag{1}$$

where k_{syn} is the synthesis rate, with dimensions of mass over time, and k_{deg} is the degradation constant, with dimensions of inverse time.

The mass *P*(t)* of enriched protein in terms of the enrichment *E(t)* at time *t*, and the precursor enrichment *E** is:

$$P^*(t) = \quad \frac{E(t)}{E^*}P(t), \tag{2}$$

The equilibrium mass P_{eq} is the constant solution $P(t) = P_{\mathrm{eq}}$ to eqn (1) for which $\mathrm{d}P/\mathrm{d}t = 0$. That is, P_{eq} is the solution to $0 = k_{\mathrm{syn}} - k_{\mathrm{deg}}P_{\mathrm{eq}}; P_{\mathrm{eq}} = k_{\mathrm{syn}}/k_{\mathrm{deg}}$. The fractional synthesis rate (FSR) = $k_{\mathrm{syn}}/P_{\mathrm{eq}}$ has dimensions of inverse time, and since $P_{\mathrm{eq}} = k_{\mathrm{syn}}/k_{\mathrm{deg}}$ is, in fact, equal to k_{deg}.

$$k_{\mathrm{deg}} = \quad -\ln\left[\left(1 - \quad \frac{E(t)}{E^*}\right)\frac{P(t)}{P^*}t\right]. \tag{3}$$

And,

$$P_{\mathrm{eq}} = \quad \frac{P^*(t)}{1 - \quad e^{-k_{\mathrm{deg}}t}} = \quad \frac{\frac{E(t)}{E^*}P(t)}{1 - \quad \left(1 - \quad \frac{E(t)}{E^*}\right)\frac{P(t)}{P_0}}. \tag{4}$$

The (nonfractional) synthesis rate k_{syn} can be obtained from eqns (3) and (4) since

$$k_{\mathrm{syn}} = \quad k_{\mathrm{deg}}P_{\mathrm{eq}}. \tag{5}$$

Protein abundance as determined by Western analysis

A portion (~30 mg) of skeletal muscle was homogenized (Bullet Blender, Next Advance, Troy, NY, USA) in 10 volumes (1:10) of ice-cold lysis buffer (100 mM NaF, 50 mM HEPES, 12 mM Sodium Pyrophosphate, 10 mM EDTA, 1% Triton x-100 by volume) supplemented with phosphatase and protease inhibitors (HALT, Thermo Fisher Scientific). Homogenized tissue was centrifuged at 16,000g for 20 minutes at 4 C°. The resulting supernatant was then diluted 1:5 in distilled water before protein content was determined by

bicinchoninic acid (BCA) assay (Thermo Fisher Scientific). Samples were then prepared in Laemmli buffer (50 mM Tris-HCl, pH 6.8, 10% glycerol, 2% SDS, 2% β-mercaptoethanol, 0.1% bromophenol blue) at a concentration of 1.5 μg/μl and boiled at 95°C for 10 minutes. After loading 15 μl of sample, proteins were then separated by SDS-PAGE using 4–15% TGX gels (Criterion, Bio-Rad, Hercules, CA, USA) by first stacking for 10 minutes at 100V, then running for ~40 minutes at 200V at room temperature. Samples were then transferred for 45 minutes at 100V on ice onto a PVDF membrane (Bio-Rad) in Towbin's buffer (25 mM Tris-base, 192 mM glycine, 20% methanol). Membranes were stained with Ponceau S (Sigma-Aldrich) and imaged, to verify transfer efficiency and equal loading among lanes. Membranes were then blocked in blocking buffer (5% nonfat dry milk in TBS-T, 20 mM Tris base, 150 mM NaCl, 0.1% Tween-20, pH 7.6) for 1 hour at room temperature, rinsed 4 × 5 min. in TBS-T, and incubated with primary antibody (in 5% BSA in TBS-T, with 0.02% NaN_3, pH 7.5) overnight at 4°C with gentle shaking. Membranes were then rinsed 4 × 5 min. in TBS-T, incubated with a secondary antibody conjugated to horseradish peroxidase (HRP) in blocking buffer for 1 hour, and rinsed 4 × 5 min. in TBS-T. HRP activity was detected by enhanced chemilumenscence substrate (SuperSignal West Dura, Thermo Fisher Scientific). Images were taken for quantification by densitometry using a FluorChem E imager (ProteinSimple, San Jose, CA). Protein content was quantified and corrected for local background using AlphaView analysis software (ProteinSimple). Individual background-corrected values were then normalized to the average optical density within the membrane for a given protein. For any proteins that contain multiple isoforms (e.g., Akt, ERK1/2, 4EBP1) we quantified all isoforms together as a single value. Membranes were then stripped (Restore Western Blot Stripping Buffer, Thermo Fisher Scientific), checked for adequate stripping, and re-probed.

FAK and p-FAK were analyzed at the University of Kentucky as previously described.[23] All other proteins were analyzed as described above at Oklahoma Medical Research Foundation. For FAK analyses, a small part of gastrocnemius muscle was homogenized in radioimmunoprecipitation assay (RIPA) buffer (Boston Bioproducts, Ashland, MA, USA) with 10μl ml^{-1} protease inhibitor cocktail (Roche, Indianapolis, IN, USA), 5 mM benzamidine, 5 mM N-ethylmaleimide, 50 mM NaF, 25 mM B-glycerophosphate, 1 mM EDTA, and 1 mM phenylmethane sulfonyl fluoride added and centrifuged at 5000g. Protein concentration of homogenates was measured using the bicinchoninic acid protein assay (BCA, Bio-Rad, Hercules, CA, USA). To measure protein abundance, 30 μg total protein was loaded and separated on 4–15% acrylamide gradient gels (Bio-Rad), followed by transfer to polyvinylidene difluoride membranes with 0.22 μm pore size (Millipore, Burlington, MA, USA). Gels intended for detection of FAK and p-FAK were transferred in 10% methanol buffer to facilitate transfer of high molecular mass proteins. Membranes were conditioned in Odyssey Blocking Buffer (Licor, Lincoln, NE, USA) followed by incubation with the appropriate primary antibody overnight at 4°C. After primary antibody incubation, membranes were washed and further reacted with highly cross-absorbed infrared-labelled secondary antibodies for 1 hour at room temperature (goat anti-rabbit (1:15,000, Licor, Lincoln, NE, USA) or goat anti-mouse (1:15,000, Invitrogen, Omaha, NE, USA)). Membranes were scanned using an Odyssey infrared imaging system (Licor) to detect

specific antibody binding and to perform quantification. Equal loading of the individual lanes was ensured by staining the membranes with Ponceau S, as described previously.[23]

Primary antibodies and dilutions used were as follows: phospho-ERK$^{Thr202/Tyr204}$ (Cell Signaling Technology; CST no. 4370, Beverly, MA, USA), 1:1000; ERK (CST no. 4695), 1:1000; phospho-Akt^{Ser473} (CST no. 4058), 1:500; Akt (CST no. 4685), 1:500; phospho-FOXO3A^{Ser235} (CST no. 9466), 1:500; FOXO3A (CST no. 12829), 1:500; phospho-eEF2^{Thr56} (CST no. 2331), 1:1000; eEF2 (CST no. 2332), 1:1000; phospho-FAK^{Tyr397} (CST no. 3283), 1:1000; FAK (CST no. 3285), 1:1000; phospho-S6K1^{Thr389} (CST no. 9234), 1:500; S6K1 (CST no. 9202), 1:1000; phospho-rpS6$^{Ser235/236}$ (CST no. 4858), 1:1000; rpS6 (CST no. 2217), 1:1000; phospho-4EBP1$^{Thr37/46}$ (CST no. 9459), 1:1000; 4EBP1 (CST no. 9452), 1:1000; MuRF-1 (ECM Biosciences no. MP3401), 1:1000; phospho-UBF-1^{Ser484} (Abcam, no. ab182583, Cambridge, MA, USA), 1:500; UBF-1 (Thermo Fisher Scientific no. PA5–36153), 1:500; and c-Myc (CST no. 13987), 1:1000. For every protein except FAK and p-FAK goat anti-rabbit, HRP-linked secondary antibody (CST no. 7074) at 1:5000 was used. The ratio of the phosphorylated over total protein is not presented here, because it is mostly determined by changes in the abundance of total proteins levels, particularly in HS, thereby artificially inflating the ratios.[23]

(Immuno)histochemistry

Myosin Heavy Chain (MyHC) determination: Mean and fiber type specific CSA was determined as previously described[23,77] with modifications for rat muscle. Briefly, 7 μm gastrocnemius muscle cross sections were retrieved from −20°C storage and left at room temperature for 1 hour. Sections were rehydrated in PBS and incubated in anti-MyHC I (1:100, BA.D5, Developmental Studies Hybridoma Bank (DHSB), Iowa City, IA), anti-MyHC IIa (1:2, SC.71, DSHB), anti-MyHC IIx (1:2, 6H1, DHSB) and anti-laminin (1:50, Sigma) overnight at 4°C. Sections were washed with PBS prior to incubation with secondary antibodies for 1 hour. Secondary antibodies goat anti-mouse IgG2b, Alexa Flour conjugated 2° antibody (1:250, Invitrogen), goat anti-mouse IgG1, Alexa Fluor 488 conjugated 2° antibody (1:500, Invitrogen), goat anti-mouse IgM, Alexa Fluor 555 conjugated 2° antibody (1:250, Invitrogen) and goat anti-rabbit IgG AMCA (1:150, Vector Laboratories) were used for anti-MyHC I, anti-MyHC IIa, anti-MyHC IIx and anti-laminin, respectively. Sections were washed, post-fixed in absolute methanol, cover slipped, and imaged using an upright fluorescent microscope (AxioImager MI, Zeiss). A total of 5 regionally representative images totaling at least 600 total muscle fibers of both medial and lateral gastrocnemius muscle were imaged and quantified for fiber type specific CSA. Quantification and fiber type distribution of laminin-outlined MyHC expressing fibers was performed using MyoVision automated analysis software as previously described;[78] MyHC IIb expressing fibers were inferred from unstained fibers.

Statistical Analyses

Massage performed during WB and HS were treated as separate experiments to independently explore massage's effects on unperturbed and disuse loading states. Both WBM and HSM experiments were performed simultaneously, although statistical comparisons were largely focused within (i.e., HS versus HSM and WB versus WBM).

However, to improve the impact of our results and interpretation, we made limited statistical comparisons of HS and HSM to WB (using ANOVA with Holm-Sidak post hoc, where appropriate) without directly showing that data side by side. Prior to any statistical analyses the data were tested for normal distribution and equal variances to determine the appropriate statistical test. For comparisons between the respective control (WB or HS) and either the massaged limb (WBM or HSM) or contralateral non-massaged limb (WBM-L or HSM-L) two-tailed independent samples t-tests were used to determine statistical significance. For fiber size frequency distribution analyses multiple t-tests for each binned fiber size were performed with a Holm-Sidak correction for multiple comparisons to determine significance across the respective control (WB or HS) and the massaged limb (WBM or HSM). All statistical analyses and figures were created using Graphpad Prism 8 (San Diego, CA, USA). All values reported are mean ± standard error (SE) and statistical significance was assumed at $p < 0.05$.

Supplementary Material

Refer to Web version on PubMed Central for supplementary material.

Acknowledgements

This work was supported by NIH grants AT009268 and AG042699 (E.D.V, T.B., B.M.). M.L. was supported by a NIA Training Grant AG052363.

REFERENCES:

1. Suetta C. Plasticity and function of human skeletal muscle in relation to disuse and rehabilitation: Influence of ageing and surgery. Dan Med J. 2017;64(8).
2. Rudrappa SS, Wilkinson DJ, Greenhaff PL, Smith K, Idris I, Atherton PJ. Human Skeletal Muscle Disuse Atrophy: Effects on Muscle Protein Synthesis, Breakdown, and Insulin Resistance-A Qualitative Review. Front Physiol. 2016;7:361. [PubMed: 27610086]
3. Phillips SM, McGlory C. CrossTalk proposal: The dominant mechanism causing disuse muscle atrophy is decreased protein synthesis. J Physiol. 2014;592(24):5341–5343. [PubMed: 25512435]
4. Reid MB, Judge AR, Bodine SC. CrossTalk opposing view: The dominant mechanism causing disuse muscle atrophy is proteolysis. J Physiol. 2014;592(24):5345–5347. [PubMed: 25512436]
5. Baehr LM, West DWD, Marshall AG, Marcotte GR, Baar K, Bodine SC. Muscle-specific and age-related changes in protein synthesis and protein degradation in response to hindlimb unloading in rats. J Appl Physiol. 2017;122(5):1336–1350. [PubMed: 28336537]
6. Ferrando AA, Lane HW, Stuart CA, Davis-Street J, Wolfe RR. Prolonged bed rest decreases skeletal muscle and whole body protein synthesis. Am J Physiol. 1996;270(4 Pt 1):E627–633. [PubMed: 8928769]
7. Gibson JN, Halliday D, Morrison WL, et al. Decrease in human quadriceps muscle protein turnover consequent upon leg immobilization. Clin Sci (Lond). 1987;72(4):503–509. [PubMed: 2435445]
8. Gibson JN, Smith K, Rennie MJ. Prevention of disuse muscle atrophy by means of electrical stimulation: maintenance of protein synthesis. Lancet. 1988;2(8614):767–770. [PubMed: 2901612]
9. Paddon-Jones D, Sheffield-Moore M, Cree MG, et al. Atrophy and impaired muscle protein synthesis during prolonged inactivity and stress. J Clin Endocrinol Metab. 2006;91(12):4836–4841. [PubMed: 16984982]
10. Wall BT, Snijders T, Senden JM, et al. Disuse impairs the muscle protein synthetic response to protein ingestion in healthy men. J Clin Endocrinol Metab. 2013;98(12):4872–4881. [PubMed: 24108315]

11. Phillips SM, Glover EI, Rennie MJ. Alterations of protein turnover underlying disuse atrophy in human skeletal muscle. J Appl Physiol. 2009;107(3):645–654. [PubMed: 19608931]
12. Glover EI, Phillips SM, Oates BR, et al. Immobilization induces anabolic resistance in human myofibrillar protein synthesis with low and high dose amino acid infusion. J Physiol. 2008;586(24):6049–6061. [PubMed: 18955382]
13. Talbert EE, Smuder AJ, Min K, Kwon OS, Powers SK. Calpain and caspase-3 play required roles in immobilization-induced limb muscle atrophy. J Appl Physiol. 2013;114(10):1482–1489. [PubMed: 23471945]
14. Huang J, Zhu X. The molecular mechanisms of calpains action on skeletal muscle atrophy. Physiol Res. 2016;65(4):547–560. [PubMed: 26988155]
15. Dupont-Versteegden EE, Strotman BA, Gurley CM, et al. Nuclear translocation of EndoG at the initiation of disuse muscle atrophy and apoptosis is specific to myonuclei. Am J Physiol Regul Integr Comp Physiol. 2006;291(6):R1730–1740. [PubMed: 16873557]
16. Vazeille E, Codran A, Claustre A, et al. The ubiquitin-proteasome and the mitochondria-associated apoptotic pathways are sequentially downregulated during recovery after immobilization-induced muscle atrophy. Am J Physiol Regul Integr Comp Physiol. 2008;295(5):E1181–1190.
17. Bonaldo P, Sandri M. Cellular and molecular mechanisms of muscle atrophy. Dis Mech Mod. 2013;6(1):25–39.
18. Sandri M Autophagy in skeletal muscle. FEBS letters. 2010;584(7):1411–1416. [PubMed: 20132819]
19. Wu CL, Kandarian SC, Jackman RW. Identification of genes that elicit disuse muscle atrophy via the transcription factors p50 and Bcl-3. PLoS One. 2011;6(1):e16171. [PubMed: 21249144]
20. Bodine SC, Baehr LM. Skeletal muscle atrophy and the E3 ubiquitin ligases MuRF1 and MAFbx/atrogin-1. Am J Physiol Endocrinol Metab. 2014;307(6):E469–484. [PubMed: 25096180]
21. Dirks ML, Wall BT, Snijders T, Ottenbros CL, Verdijk LB, van Loon LJ. Neuromuscular electrical stimulation prevents muscle disuse atrophy during leg immobilization in humans. Acta Physiol. 2014;210(3):628–641.
22. Haddad F, Adams GR, Bodell PW, Baldwin KM. Isometric resistance exercise fails to counteract skeletal muscle atrophy processes during the initial stages of unloading. J Appl Physiol. 2006;100(2):433–441. [PubMed: 16239603]
23. Miller BF, Hamilton KL, Majeed ZR, et al. Enhanced skeletal muscle regrowth and remodelling in massaged and contralateral non-massaged hindlimb. J Physiol. 2018;596(1):83–103. [PubMed: 29090454]
24. Waters-Banker C, Butterfield TA, Dupont-Versteegden EE. Immunomodulatory effects of massage on nonperturbed skeletal muscle in rats. J Appl Physiol. 2014;116(2):164–175. [PubMed: 24201707]
25. Van Pelt DW, Confides AL, Abshire SM, Hunt ER, Dupont-Versteegden EE, Butterfield TA. Age-related responses to a bout of mechanotherapy in skeletal muscle of rats. J Appl Physiol. 2019;127(6):1782–1791. [PubMed: 31670600]
26. Miller BF, Wolff CA, Peelor FF 3rd, Shipman PD, Hamilton KL. Modeling the contribution of individual proteins to mixed skeletal muscle protein synthetic rates over increasing periods of label incorporation. J Appl Physiol. 2015;118(6):655–661. [PubMed: 25593288]
27. Cholewa JM, Dardevet D, Lima-Soares F, et al. Dietary proteins and amino acids in the control of the muscle mass during immobilization and aging: role of the MPS response. Amino Acids. 2017;49(5):811–820. [PubMed: 28175999]
28. Chaillou T, Kirby TJ, McCarthy JJ. Ribosome biogenesis: emerging evidence for a central role in the regulation of skeletal muscle mass. J Cell Physiol. 2014;229(11):1584–1594. [PubMed: 24604615]
29. Figueiredo VC, McCarthy JJ. Regulation of Ribosome Biogenesis in Skeletal Muscle Hypertrophy. Physiology. 2019;34(1):30–42. [PubMed: 30540235]
30. Saxton RA, Sabatini DM. mTOR Signaling in Growth, Metabolism, and Disease. Cell. 2017;168(6):960–976. [PubMed: 28283069]

31. Nader GA, McLoughlin TJ, Esser KA. mTOR function in skeletal muscle hypertrophy: increased ribosomal RNA via cell cycle regulators. Am J Physiol Cell Physiol. 2005;289(6):C1457–1465. [PubMed: 16079186]
32. von Walden F, Casagrande V, Ostlund Farrants AK, Nader GA. Mechanical loading induces the expression of a Pol I regulon at the onset of skeletal muscle hypertrophy. Am J Physiol Cell Physiol. 2012;302(10):C1523–1530. [PubMed: 22403788]
33. von Walden F, Liu C, Aurigemma N, Nader GA. mTOR signaling regulates myotube hypertrophy by modulating protein synthesis, rDNA transcription, and chromatin remodeling. Am J Physiol Cell Physiol. 2016;311(4):C663–C672. [PubMed: 27581648]
34. McDermott PJ, Carl LL, Conner KJ, Allo SN. Transcriptional regulation of ribosomal RNA synthesis during growth of cardiac myocytes in culture. J Biol Chem. 1991;266(7):4409–4416. [PubMed: 1999424]
35. McDermott PJ, Rothblum LI, Smith SD, Morgan HE. Accelerated rates of ribosomal RNA synthesis during growth of contracting heart cells in culture. J Biol Chem. 1989;264(30):18220–18227. [PubMed: 2808374]
36. Goodman CA, Frey JW, Mabrey DM, et al. The role of skeletal muscle mTOR in the regulation of mechanical load-induced growth. J Physiol. 2011;589(Pt 22):5485–5501. [PubMed: 21946849]
37. Nakada S, Ogasawara R, Kawada S, Maekawa T, Ishii N. Correlation between Ribosome Biogenesis and the Magnitude of Hypertrophy in Overloaded Skeletal Muscle. PLoS One. 2016;11(1):e0147284. [PubMed: 26824605]
38. Stec MJ, Kelly NA, Many GM, Windham ST, Tuggle SC, Bamman MM. Ribosome biogenesis may augment resistance training-induced myofiber hypertrophy and is required for myotube growth in vitro. Am J Physiol Endocrinol Metab. 2016;310(8):E652–E661. [PubMed: 26860985]
39. Sieljacks P, Wang J, Gronnebaek T, et al. Six Weeks of Low-Load Blood Flow Restricted and High-Load Resistance Exercise Training Produce Similar Increases in Cumulative Myofibrillar Protein Synthesis and Ribosomal Biogenesis in Health Males. Front Physiol. 2019.
40. Babij P, Booth FW. Alpha-actin and cytochrome c mRNAs in atrophied adult rat skeletal muscle. Am J Physiol. 1988;254(5 Pt 1):C651–656. [PubMed: 2834956]
41. Gamrin L, Berg HE, Essen P, et al. The effect of unloading on protein synthesis in human skeletal muscle. Acta Physiol. 1998;163(4):369–377.
42. Haddad F, Baldwin KM, Tesch PA. Pretranslational markers of contractile protein expression in human skeletal muscle: effect of limb unloading plus resistance exercise. J Appl Physiol. 2005;98(1):46–52. [PubMed: 15298986]
43. Heinemeier KM, Olesen JL, Haddad F, Schjerling P, Baldwin KM, Kjaer M. Effect of unloading followed by reloading on expression of collagen and related growth factors in rat tendon and muscle. J Appl Physiol. 2009;106(1):178–186. [PubMed: 18988763]
44. Petersson B, Wernerman J, Waller SO, von der Decken A, Vinnars E. Elective abdominal surgery depresses muscle protein synthesis and increases subjective fatigue: effects lasting more than 30 days. Br J Surg. 1990;77(7):796–800. [PubMed: 2383755]
45. You JS, Anderson GB, Dooley MS, Hornberger TA. The role of mTOR signaling in the regulation of protein synthesis and muscle mass during immobilization in mice. Dis Mech Model. 2015;8(9):1059–1069.
46. Mathis AD, Naylor BC, Carson RH, et al. Mechanisms of In Vivo Ribosome Maintenance Change in Response to Nutrient Signals. Mol Cell Prot : MCP. 2017;16(2):243–254.
47. Miller BF, Baehr LM, Musci RV, et al. Muscle-specific changes in protein synthesis with aging and reloading after disuse atrophy. J Cachex Sarcopenia Muscle. 2019.
48. Bederman IR, Lai N, Shuster J, Henderson L, Ewart S, Cabrera ME. Chronic hindlimb suspension unloading markedly decreases turnover rates of skeletal and cardiac muscle proteins and adipose tissue triglycerides. J Appl Physiol. 2015;119(1):16–26. [PubMed: 25930021]
49. Samarel AM. In vivo measurements of protein turnover during muscle growth and atrophy. FASEB J. 1991;5(7):2020–2028. [PubMed: 2010055]
50. Thomason DB, Booth FW. Atrophy of the soleus muscle by hindlimb unweighting. J Appl Physiol. 1990;68(1):1–12. [PubMed: 2179205]

51. Butterfield TA, Zhao Y, Agarwal S, Haq F, Best TM. Cyclic compressive loading facilitates recovery after eccentric exercise. Med Sci Sport Exerc. 2008;40(7):1289–1296.
52. Crawford SK, Haas C, Butterfield TA, et al. Effects of immediate vs. delayed massage-like loading on skeletal muscle viscoelastic properties following eccentric exercise. Clin Biomech (Bristol, Avon). 2014;29(6):671–678.
53. Haas C, Butterfield TA, Abshire S, et al. Massage timing affects postexercise muscle recovery and inflammation in a rabbit model. Med Sci Sport Exerc. 2013;45(6):1105–1112.
54. Haas C, Butterfield TA, Zhao Y, Zhang X, Jarjoura D, Best TM. Dose-dependency of massage-like compressive loading on recovery of active muscle properties following eccentric exercise: rabbit study with clinical relevance. Br J Sports Med. 2013;47(2):83–88. [PubMed: 22736207]
55. Kirby TJ, Lee JD, England JH, Chaillou T, Esser KA, McCarthy JJ. Blunted hypertrophic response in aged skeletal muscle is associated with decreased ribosome biogenesis. J Appl Physiol. 2015;119(4):321–327. [PubMed: 26048973]
56. West DWD, Marcotte GR, Chason CM, et al. Normal Ribosomal Biogenesis but Shortened Protein Synthetic Response to Acute Eccentric Resistance Exercise in Old Skeletal Muscle. Front Physiol. 2018;9:1915. [PubMed: 30692935]
57. Brook MS, Wilkinson DJ, Mitchell WK, et al. A novel D2O tracer method to quantify RNA turnover as a biomarker of de novo ribosomal biogenesis, in vitro, in animal models, and in human skeletal muscle. Am J Physiol Endocrinol Metab. 2017;313(6):E681–E689. [PubMed: 28811296]
58. Millward DJ, Garlick PJ, James WP, Nnanyelugo DO, Ryatt JS. Relationship between protein synthesis and RNA content in skeletal muscle. Nature. 1973;241(5386):204–205. [PubMed: 4700888]
59. Baehr LM, West DW, Marcotte G, et al. Age-related deficits in skeletal muscle recovery following disuse are associated with neuromuscular junction instability and ER stress, not impaired protein synthesis. Aging (Albany NY). 2016;8(1):127–146. [PubMed: 26826670]
60. Gordon SE, Fluck M, Booth FW. Selected Contribution: Skeletal muscle focal adhesion kinase, paxillin, and serum response factor are loading dependent. J Appl Physiol. 2001;90(3):1174–1183; discussion 1165. [PubMed: 11181634]
61. Thomson DM, Fick CA, Gordon SE. AMPK activation attenuates S6K1, 4E-BP1, and eEF2 signaling responses to high-frequency electrically stimulated skeletal muscle contractions. J Appl Physiol. 2008;104(3):625–632. [PubMed: 18187610]
62. Baar K, Esser K. Phosphorylation of p70(S6k) correlates with increased skeletal muscle mass following resistance exercise. Am J Physiol. 1999;276(1 Pt 1):C120–127. [PubMed: 9886927]
63. Carroll TJ, Herbert RD, Munn J, Lee M, Gandevia SC. Contralateral effects of unilateral strength training: evidence and possible mechanisms. J Appl Physiol. 2006;101(5):1514–1522. [PubMed: 17043329]
64. Munn J, Herbert RD, Gandevia SC. Contralateral effects of unilateral resistance training: a meta-analysis. J Appl Physiol. 2004;96(5):1861–1866. [PubMed: 15075311]
65. Munn J, Herbert RD, Hancock MJ, Gandevia SC. Training with unilateral resistance exercise increases contralateral strength. J Appl Physiol. 2005;99(5):1880–1884. [PubMed: 16024518]
66. Andrushko JW, Gould LA, Farthing JP. Contralateral effects of unilateral training: sparing of muscle strength and size after immobilization. Appl Physiol Nutr Metab. 2018;43(11):1131–1139. [PubMed: 29800529]
67. Andrushko JW, Lanovaz JL, Bjorkman KM, Kontulainen SA, Farthing JP. Unilateral strength training leads to muscle-specific sparing effects during opposite homologous limb immobilization. J Appl Physiol. 2018;124(4):866–876. [PubMed: 29357520]
68. Ruddy KL, Carson RG. Neural pathways mediating cross education of motor function. Front Hum Neurosci. 2013;7:397. [PubMed: 23908616]
69. Whitham M, Parker BL, Friedrichsen M, et al. Extracellular Vesicles Provide a Means for Tissue Crosstalk during Exercise. Cell Metab. 2018;27(1):237–251 e234. [PubMed: 29320704]
70. Persson PB. Good publication practice in physiology 2019. Acta Physiol. 2019;227(4):e13405.
71. White JR, Confides AL, Moore-Reed S, Hoch JM, Dupont-Versteegden EE. Regrowth after skeletal muscle atrophy is impaired in aged rats, despite similar responses in signaling pathways. Exp Gerontol. 2015;64:17–32. [PubMed: 25681639]

72. Hunt ER, Confides AL, Abshire SM, Dupont-Versteegden EE, Butterfield TA. Massage increases satellite cell number independent of the age-associated alterations in sarcolemma permeability. Physiol Rep. 2019;7(17):e14200. [PubMed: 31496052]

73. Drake JC, Bruns DR, Peelor FF 3rd, et al. Long-lived crowded-litter mice have an age-dependent increase in protein synthesis to DNA synthesis ratio and mTORC1 substrate phosphorylation. Am J Physiol Endocrinol Metab. 2014;307(9):E813–821. [PubMed: 25205819]

74. Drake JC, Bruns DR, Peelor FF 3rd, et al. Long-lived Snell dwarf mice display increased proteostatic mechanisms that are not dependent on decreased mTORC1 activity. Aging Cell. 2015;14(3):474–482. [PubMed: 25720574]

75. Drake JC, Peelor FF 3rd, Biela LM, et al. Assessment of mitochondrial biogenesis and mTORC1 signaling during chronic rapamycin feeding in male and female mice. J Gerontol A Biol Sci Med Sci. 2013;68(12):1493–1501. [PubMed: 23657975]

76. Busch R, Kim YK, Neese RA, et al. Measurement of protein turnover rates by heavy water labeling of nonessential amino acids. Biochim Biophys Acta. 2006;1760(5):730–744. [PubMed: 16567052]

77. Murach KA, Confides AL, Ho A, et al. Depletion of Pax7+ satellite cells does not affect diaphragm adaptations to running in young or aged mice. J Physiol. 2017;595(19):6299–6311. [PubMed: 28736900]

78. Wen Y, Murach KA, Vechetti IJ Jr., et al. MyoVision: software for automated high-content analysis of skeletal muscle immunohistochemistry. J Appl Physiol. 2018;124(1):40–51. [PubMed: 28982947]

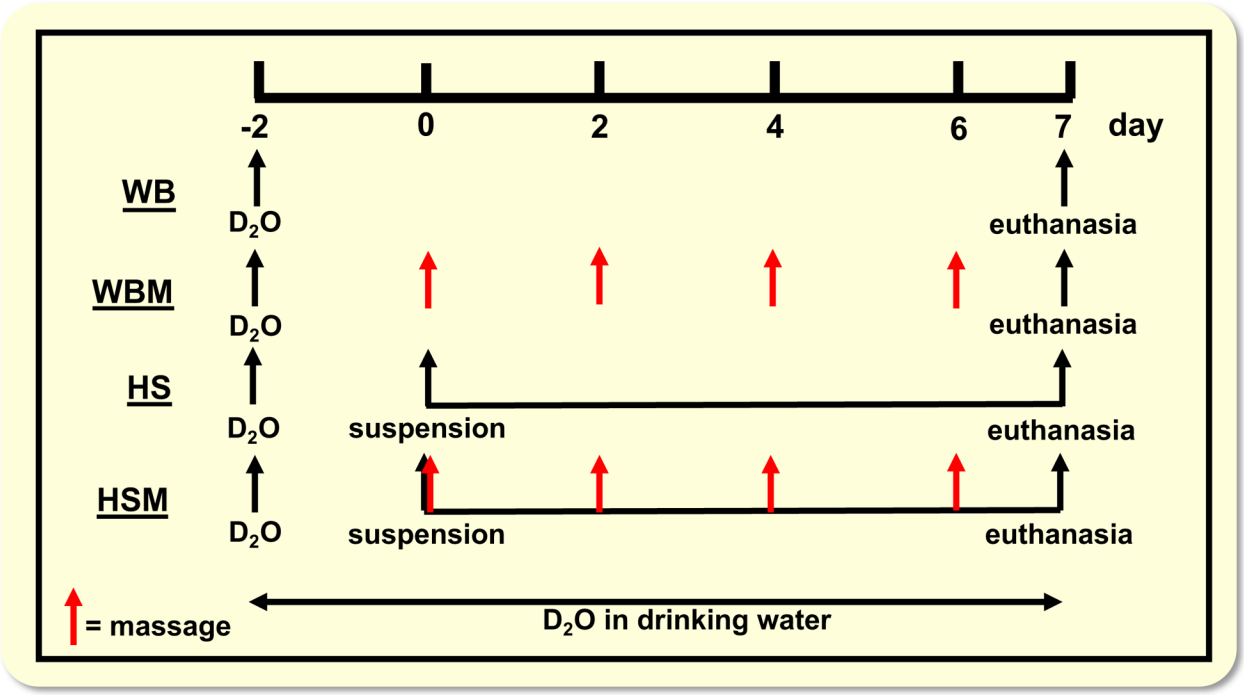

Figure 1.

Overview of experimental design. WB, weight bearing; WBM, weight bearing with massage through CCL (indicated with red arrows); HS, hindlimb suspension; HSM, hindlimb suspension with massage through CCL. D_2O indicates time points of heavy water injections. Rats received D_2O in drinking water after the injections until euthanasia.

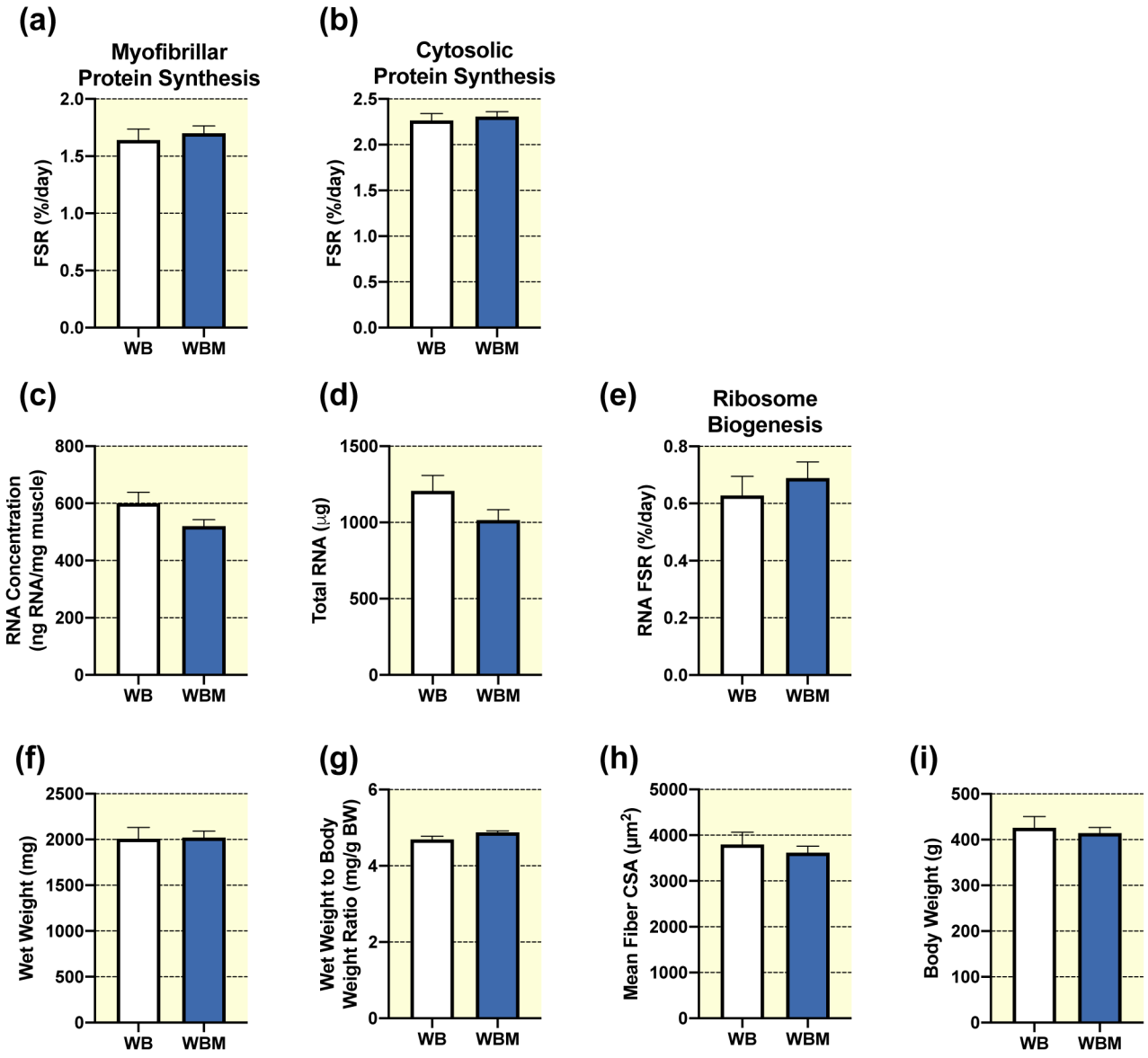

Figure 2. Massage during normal ambulatory weight bearing (WB) has no effect on protein synthesis, ribosomal biogenesis, and muscle mass or size in the massaged limb.

Gastrocnemius myofibrillar (a) and cytosolic (b) fractional synthesis rate (FSR), RNA concentration (c), total RNA (d), RNA FSR (e), wet weight (f), wet weight to body weight ratio (g), and quantification of mean fiber CSA (h) from gastrocnemius muscles of WB (n=8) and WB massaged limb, WBM (n=9). Also, body weights (i) from WB and WBM animals, respectively. Values are mean ± SEM. Two-tailed independent samples t-tests were used to determine statistical significance between WB and WBM: $p < 0.05$.

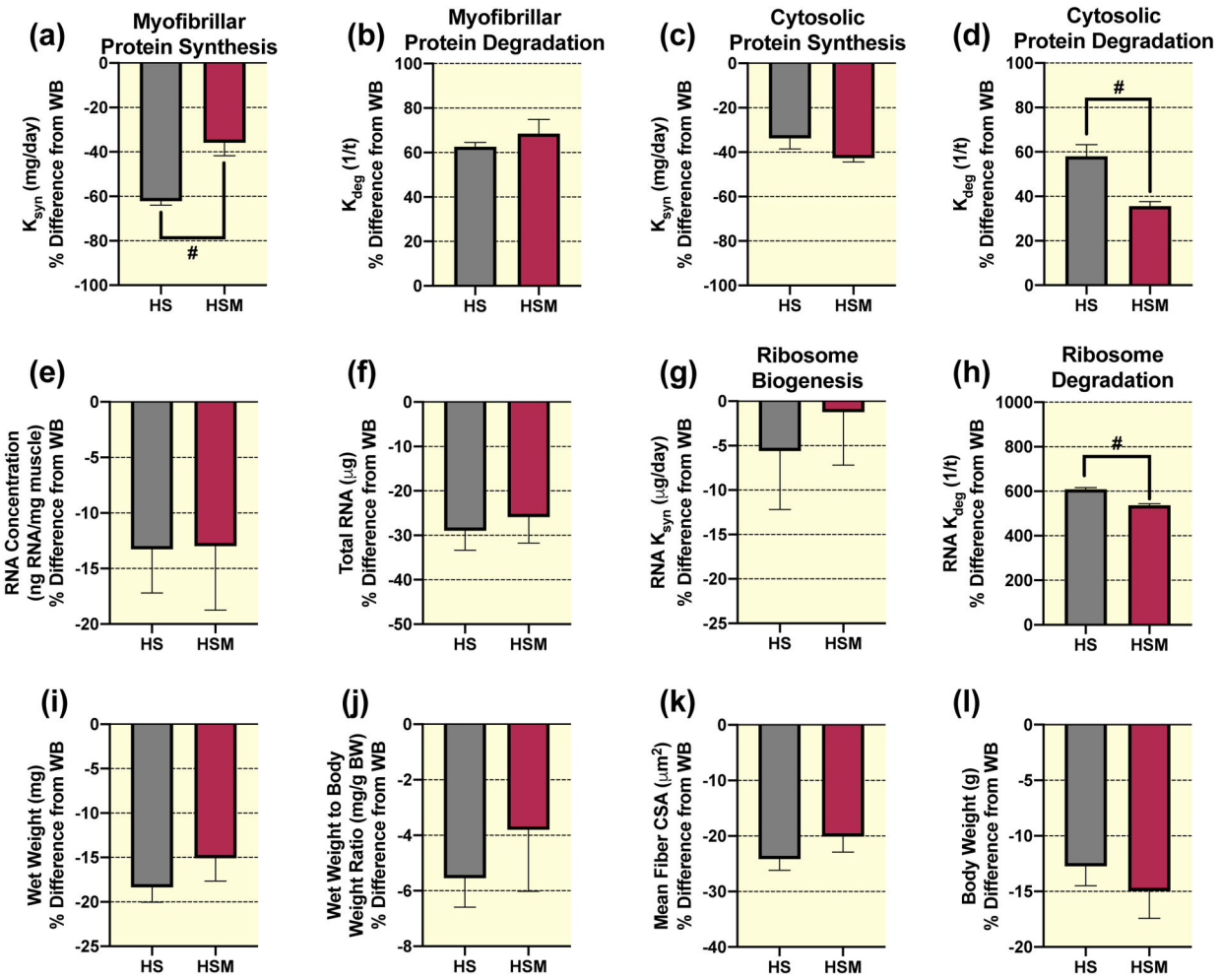

Figure 3. Massage during hindlimb suspension (HS) alters myofibrillar and cytosolic protein turnover, and ribosome turnover, without any effect on muscle size.

Calculated myofibrillar K_{syn} (a), myofibrillar K_{deg} (b), cytosolic K_{syn} (c), and cytosolic K_{deg} (d), RNA concentration (e), total RNA (f), RNA K_{syn} (g), RNA K_{deg} (h), wet weight (i), wet weight to body weight ratio (j), and mean fiber CSA (k) percent (%) difference from weight bearing (WB) from gastrocnemius muscles of HS (n=8) and HS massaged limb, HSM (n=9). Also, body weight percent difference from WB in HS and HSM animals (l), respectively. Values are mean ± SEM. Independent samples t-tests were used to determine statistical significance between HS and HSM: #different from HS, $p < 0.05$.

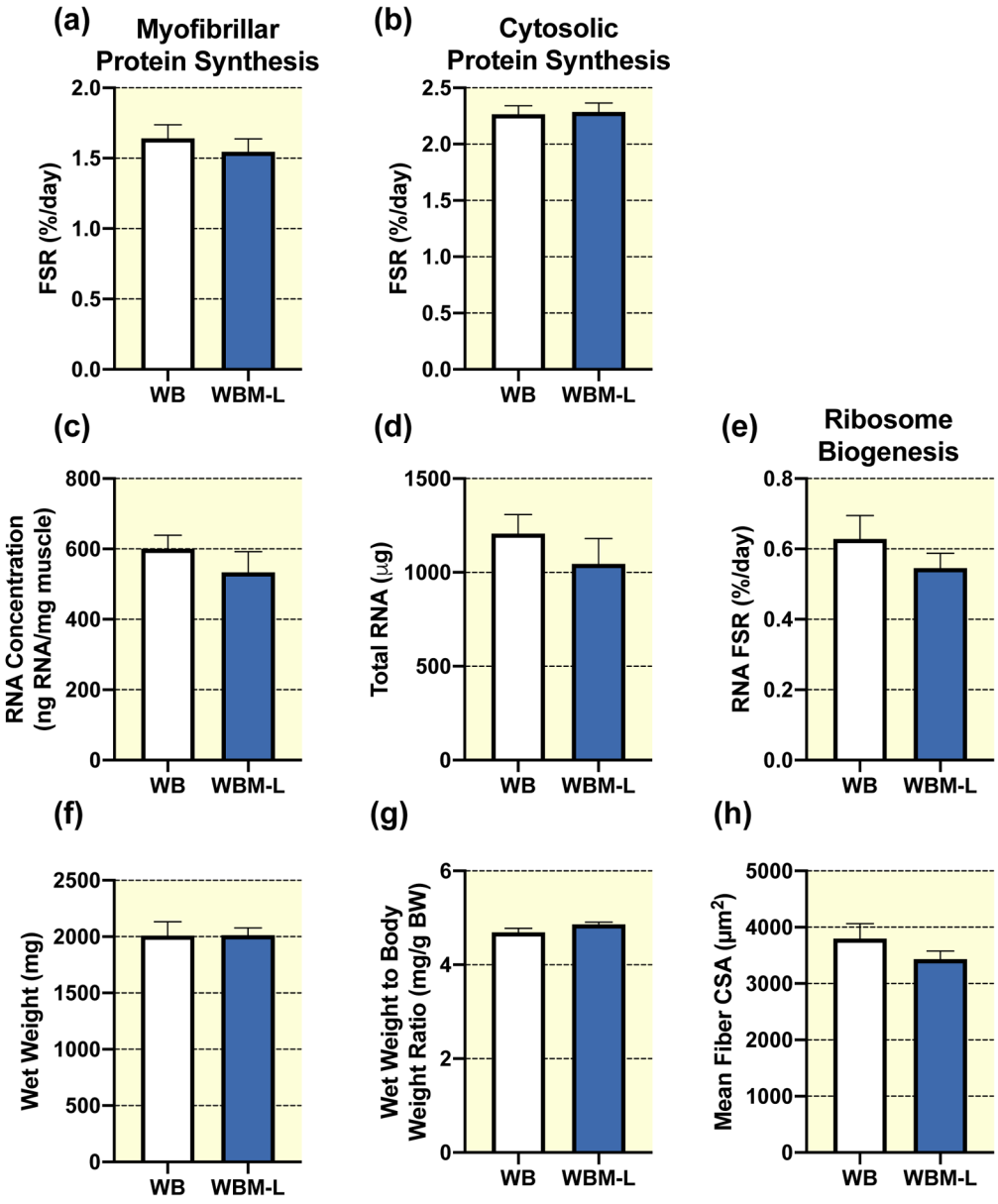

Figure 4. Massage during normal ambulatory weight bearing (WB) has no effect on protein synthesis, ribosomal biogenesis, and muscle mass or size in the contralateral non-massaged limb (WBM-L).

Gastrocnemius myofibrillar (a) and cytosolic (b) fractional synthesis rate (FSR), RNA concentration (c), total RNA (d), RNA FSR (e), wet weight (f), wet weight to body weight ratio (g), and quantification of mean fiber CSA (h) from gastrocnemius muscles of WB (n=8) and the WB contralateral non-massaged limb, WBM-L (n=9). Values are mean ± SEM. Two-tailed independent samples t-tests between the respective control (WB) and the contralateral non-massaged limb (WBM-L) were used to determine statistical significance: $p < 0.05$.

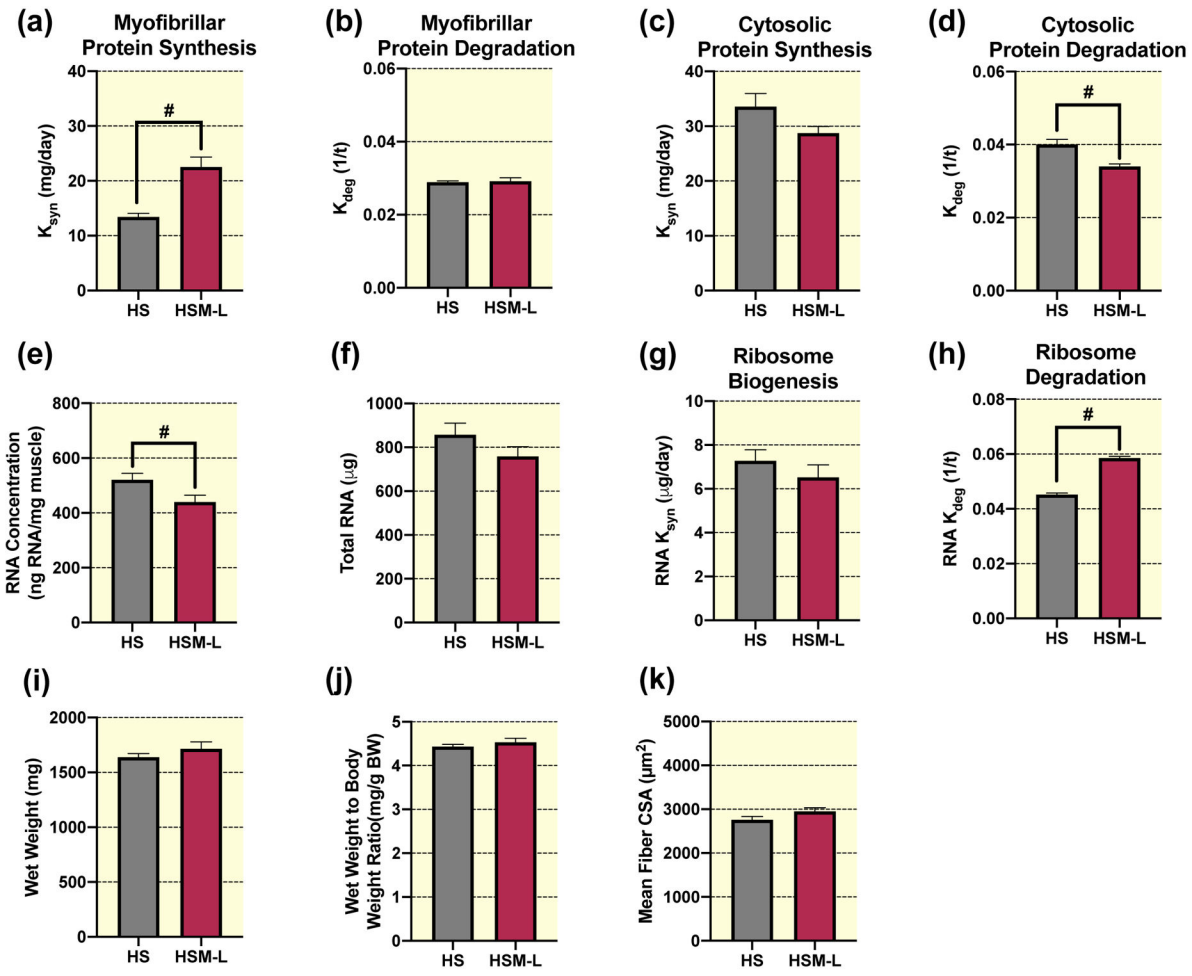

Figure 5. Massage during hindlimb suspension (HS) stimulates myofibrillar and cytosolic protein turnover, and ribosome turnover, without any effect on muscle mass or size in the contralateral non-massaged limb (HSM-L).

Calculated myofibrillar K_{syn} (a), myofibrillar K_{deg} (b), cytosolic K_{syn} (c), and cytosolic K_{deg} (d), RNA concentration (e), total RNA (f), RNA K_{syn} (g), RNA K_{deg} (h), wet weight (i), wet weight to body weight ratio (j), and quantification of mean fiber CSA (k) absolute values from gastrocnemius muscles of HS (n=8) and the contralateral non-massaged limb, HSM-L (n=9). Values are mean ± SEM. Independent samples t-tests were used to determine statistical significance between HS and HSM-L: #different from HS, $p < 0.05$.

Table 1.

Gastrocnemius fiber type CSA in massaged limb (WBM or HSM) and contralateral non-massaged limb (WBM-L or HSM-L) in response to massage.

Cross-sectional area (CSA) for individual fiber types were quantified from gastrocnemius cross-sections in μm^2, from WB (n=8), WB massaged limb WBM (n=9), HS (n=8), HS massaged limb HSM (n=9), WB non-massaged contralateral limb WBM-L (n=9), and HS non-massaged contralateral limb HSM-L (n=9). Values are mean ± SEM. Two-tailed independent samples t-tests between the respective control (WB or HS) and either the massaged limb (WBM or HSM) or contralateral non-massaged limb (WBM-L or HSM-L) were used to determine statistical significance.

	WB	WBM	HS	HSM	WBM-L	HSM-L
Type I	2112 ± 104	1965 ± 265	1699 ± 138	1576 ± 99	1981 ± 125	1877 ± 118
Type IIA	2026 ± 108	2099 ± 183	1451 ± 84	1480 ± 108	1965 ± 175	1547 ± 76
Type IIX	3251 ± 143	3203 ± 287	2273 ± 101	2457 ± 141	3241 ± 176	2518 ± 178
Type IIB	4905 ± 101	4970 ± 400	3662 ± 141	3639 ± 173	4551 ± 247	3872 ± 187
Hybrid	3793 ± 747	2518 ± 327	2345 ± 471	1740 ± 226	2741 ± 373	1812 ± 186

CSA measured in μm^2. Values are means ± SEM.

Table 2.

Gastrocnemius fiber type distribution in massaged limb (WBM or HSM) and contralateral non-massaged limb (WBM-L or HSM-L) in response to massage.

Individual fiber type distribution given as percentages (%) were quantified from gastrocnemius cross-sections, from WB (n=8), WB massaged limb WBM (n=9), HS (n=8), HS massaged limb HSM (n=9), WB non-massaged contralateral limb WBM-L (n=9), and HS non-massaged contralateral limb HSM-L (n=9). Values are mean ± SEM. Two-tailed independent samples t-tests between the respective control (WB or HS) and either the massaged limb (WBM or HSM) or contralateral non-massaged limb (WBM-L or HSM-L) were used to determine statistical significance.

	WB	WBM	HS	HSM	WBM-L	HSM-L
Type I	7.9 ± 1.4	6.3 ± 0.9	6.8 ± 1.3	9.0 ± 1.4	10.1 ± 1.1	6.8 ± 1.4
Type IIA	9.9 ± 1.4	8.6 ± 1.2	7.8 ± 1.1	8.5 ± 1.1	9.9 ± 0.9	9.0 ± 3.2
Type IIX	47.0 ± 5.7	45.2 ± 4.2	45.1 ± 5.0	41.2 ± 4.4	45.7 ± 4.9	47.9 ± 6.9
Type IIB	33.8 ± 5.8	38.1 ± 4.8	39.5 ± 4.6	39.9 ± 4.8	33.3 ± 5.0	34.9 ± 6.1
Hybrid	1.4 ± 0.5	1.8 ± 0.5	0.9 ± 0.2	1.3 ± 0.3	1.0 ± 0.2	2.5 ± 1.7

Fiber type distribution given as percentages (%). Values are means ± SEM.

Table 3.

Western blot analysis of intracellular signaling pathways in massaged limb (WBM or HSM) and contralateral non-massaged limb (WBM-L or HSM-L) in response to massage.

Total and phosphorylated analysis of signaling proteins from WB (n=8), WB massaged limb WBM (n=9), HS (n=8), HS massaged limb HSM (n=9), WB non-massaged contralateral limb WBM-L (n=9), and HS non-massaged contralateral limb HSM-L (n=9). All values are in arbitrary density units. Values are mean ± SEM. Two-tailed independent samples t-tests between the respective control (WB or HS) and either the massaged limb (WBM or HSM) or contralateral non-massaged limb (WBM-L or HSM-L) were used to determine statistical significance: *different from WB, #different from HS, $p < 0.05$. Representative images for the data within this table are in Supplemental Figure 5.

	WB	WBM	HS	HSM	WBM-L	HSM-L
Total Akt	0.90 ± 0.06	0.80 ± 0.04	0.76 ± 1.00	0.96 ± 0.05	0.62 ± 0.04 *	0.86 ± 0.06
Phospho-Akt	0.86 ± 0.05	0.98 ± 0.08	0.90 ± 0.11	0.99 ± 0.13	0.83 ± 0.08	0.80 ± 0.08
Total FOXO3A	0.92 ± 0.08	0.90 ± 0.07	0.92 ± 0.10	0.99 ± 0.07	1.02 ± 0.07	1.05 ± 0.08
Phospho-FOXO3A	0.83 ± 0.05	0.78 ± 0.05	0.85 ± 0.04	0.83 ± 0.04	0.73 ± 0.04	0.82 ± 0.07
Total FAK	2.70 ± 0.31	3.80 ± 0.55	3.70 ± 0.26	4.20 ± 0.44	3.80 ± 0.39	4.20 ± 0.26
Phospho-FAK	0.80 ± 0.14	0.96 ± 0.08	0.92 ± 0.09	0.88 ± 0.08	0.82 ± 0.10	0.89 ± 0.06
Total ERK1/2	0.84 ± 0.07	0.87 ± 0.03	0.82 ± 0.06	0.89 ± 0.05	0.86 ± 0.04	0.88 ± 0.05
Phospho-ERK1/2	0.91 ± 0.04	0.89 ± 0.04	0.95 ± 0.06	0.94 ± 0.05	0.90 ± 0.05	0.95 ± 0.06
Total eEF2	0.85 ± 0.06	0.85 ± 0.05	1.00 ± 0.14	0.91 ± 0.10	0.90 ± 0.05	0.91 ± 0.09
Phospho-eEF2	0.91 ± 0.12	0.91 ± 0.07	0.98 ± 0.07	0.97 ± 0.07	0.96 ± 0.09	0.96 ± 0.04
Total S6K1	0.83 ± 0.06	0.92 ± 0.05	0.94 ± 0.03	1.05 ± 0.05	1.04 ± 0.05 *	0.95 ± 0.06
Phospho-S6K1	0.68 ± 0.13	0.83 ± 0.16	0.39 ± 0.07	0.62 ± 0.16	1.00 ± 0.15	0.68 ± 0.13
Total 4EBP1	0.79 ± 0.05	0.83 ± 0.05	1.00 ± 0.08	1.10 ± 0.06	0.89 ± 0.04	1.10 ± 0.05
Phospho-4EBP1	0.88 ± 0.08	0.82 ± 0.09	1.10 ± 0.08	1.10 ± 0.12	0.93 ± 0.10	1.30 ± 0.07
Total rpS6	1.07 ± 0.11	1.00 ± 0.09	1.15 ± 0.12	1.10 ± 0.06	1.06 ± 0.06	1.07 ± 0.07
Phospho-rpS6	0.87 ± 0.16	0.73 ± 0.18	0.73 ± 0.13	0.95 ± 0.23	0.94 ± 0.13	1.39 ± 0.20 #
Total MuRF1	0.89 ± 0.07	0.94 ± 0.07	0.90 ± 0.06	0.92 ± 0.05	1.02 ± 0.06	1.03 ± 0.08
Total UBF-1	1.00 ± 0.11	1.20 ± 0.11	1.03 ± 0.08	1.20 ± 0.11	1.40 ± 0.07 *	1.24 ± 0.07
Phospho UBF-1	0.94 ± 0.05	0.90 ± 0.08	0.84 ± 0.08	0.85 ± 0.09	0.96 ± 0.05	0.91 ± 0.09
Total c-Myc	0.73 ± 0.11	0.68 ± 0.11	0.72 ± 0.05	1.04 ± 0.14 #	0.74 ± 0.08	0.95 ± 0.09

All values are in arbitrary density units. Values are means ± SEM.

*Different from WB.

#Different from HS.